Entropy Coding Aided Adaptive Subcarrier-Index Modulated OFDM

MOHAMMAD ISMAT KADIR[1], HONGMING ZHANG[2], (Student Member, IEEE), SHENG CHEN[2], (Fellow, IEEE), AND LAJOS HANZO [2], (Fellow, IEEE)

[1]Electronics and Communication Engineering Discipline, Khulna University, Khulna 9208, Bangladesh
[2]School of Electronics and Computer Science, University of Southampton, Southampton SO17 1BJ, U.K.

Corresponding author: Lajos Hanzo (lh@ecs.soton.ac.uk)

ABSTRACT We propose entropy coding-aided adaptive subcarrier-index-modulated orthogonal frequency division multiplexing (SIM-OFDM). In conventional SIM-OFDM, the indices of the subcarriers activated are capable of conveying extra information. We propose the novel concept of compressing the index information bits by employing the Huffman coding. The probabilities of the different subcarrier activation patterns are obtained from an optimization procedure, which improves the performance of the scheme. Both the maximum-likelihood as well as the logarithmic-likelihood ratio-based soft detector may be employed for detecting the subcarriers activated as well as the information mapped to the classic constellation symbols. As an additional advantage of employing the variable-length Huffman codebook, all the legitimate subcarrier activation patterns may be employed, whereas the conventional SIM-OFDM is capable of using only a subset of the patterns. Our simulation results show that an improved performance is attainable by the proposed system.

INDEX TERMS Orthogonal frequency division multiplexing (OFDM), subcarrier index modulation-orthogonal frequency division multiplexing (SIM-OFDM), entropy coding, capacity, energy-efficiency (EE).

I. INTRODUCTION

Orthogonal frequency division multiplexing (OFDM) was conceived in the 1960s [1], [2], and it was included in numerous standards conceived for diverse applications [3]–[5]. The rudimentary idea behind OFDM transmission is to partition the transmit bitstream into many low-rate bitstreams, which are transmitted in parallel over different frequency subchannels. As a result, the transmission rate of each subchannel is considerably reduced and the subchannel bandwidth becomes much lower than the overall system's bandwidth. As a benefit, each of the individual subchannel signals experiences frequency-flat fading. Additionally, the inter-symbol interference (ISI) imposed by dispersive channels can be mitigated by introducing a sufficiently long cyclic prefix (CP). The most important aspect which made OFDM attractive is that the digital implementation of OFDM employing the discrete Fourier transform (DFT) is convenient [2]. On the other hand, a new research idea namely subcarrier-index modulated (SIM-) OFDM [6]–[9] has emerged, which activates only a specified limited number of OFDM subcarriers, rather than activating all the OFDM subcarriers during any of the OFDM symbol durations. Some of the source bits are mapped to

the indices of the activated subcarriers in addition to the bits mapped to the classic constellation symbols. The first SIM-aided OFDM study was carried out in [6], where the concept was termed as the 'parallel combinatory OFDM' (PC-OFDM) and it was subsequently followed by [10]–[15]. The bits mapped to the subcarrier indices of the PC-OFDM system were referred to as the PC bits. The PC-OFDM was also employed for optical wireless systems in [10]. Later SIM-OFDM was also proposed [13], which was capable of exploiting the subcarrier index to carry information bits similarly to spatial modulation (SM) [16]–[18], where additional information is carried by the antenna element (AE) index or the spatial index. The detailed transceiver architecture of the SIM-OFDM system was provided in [7]–[9] and was extended to the SIM-aided multiple-input multiple-output (MIMO)-OFDM scenario in [15]. A detailed analysis of the achievable rate of the SIM-OFDM employing both the localized and the interleaved subcarrier grouping method was carried out in [14]. Compressed sensing was also invoked both at the encoder and the decoder of the SIM-OFDM system [19] in order to improve its performance.

The SIM-OFDM schemes referred to above deal with the mapping of the subcarrier index bits to the set of subcarriers activated with equal probabilities, regardless of the instantaneous channel quality. However, for reliable, energy-efficient and spectrally efficient wireless transmissions, the adaptation of the access technology to the time-variant channel state is of vital importance [20], [21]. To achieve high system capacity even in time-variant channel conditions, adaptive antenna selection was studied in [22] and [23] in the context of MIMO systems. Energy-aware space-shift-keying (SSK) MIMO utilizing optimized power allocation for the activated AEs was proposed in [24] and [25]. Furthermore, the activation of the appropriate AE for providing both capacity-optimal as well as error-performance-optimal transmissions in SM-based MIMO systems was investigated in [26]–[28]. An adaptive channel-aware modulation scheme was conceived for different OFDM subcarriers [29]–[31] and a capacity-maximizing adaptive subcarrier selection was proposed in [32]. A plethora of algorithms is available in the literature for the subcarrier and power allocation of multiuser OFDM or for orthogonal frequency division multiple access (OFDMA) systems, for example [33]–[35]. It is thus imperative to conceive new OFDM-based systems which will be adaptive to the time-variant channel conditions.

A subcarrier allocation scheme or subcarrier grouping method based on the subcarrier index bits has been proposed in [36] for improving the performance of SIM-OFDM systems. On the other hand, an energy-efficient SSK transmission scheme employing the Huffman coding [37] principle was proposed in [25], where the source bits are mapped to the transmit AEs of a MIMO system based on the probabilities obtained by an energy-efficiency (EE) optimization procedure. As a further advance, an adaptive SM scheme relying on Huffman coding was also proposed [38], where the activated transmit AEs carry source information mapped to the $\mathcal{L}$-phase shift keying (PSK)/quadrature amplitude modulation (QAM) symbols in addition to the bits mapped to the transmit AE indices in accordance with probabilities gleaned from an optimization procedure. To be more specific, in contrast to the conventional SM-MIMO [16], [17] where the source bits are mapped to the classic $\mathcal{L}$-PSK/QAM symbols as well as to the AE indices with equal probability, the adaptive SM scheme of [38] attaches different probabilties of being mapped to different AEs and these probabilities are obtained from an optimization procedure formulated either for maximizing the capacity or for minimizing the symbol error rate (SER), depending on the near-instantaneous channel conditions. The AE index bits are mapped to the activated AEs by Huffman coding using the above-mentioned probabilities. Since the SIM-OFDM system [7], [9] is in principle similar to the SM scheme, where additional implicit bits are mapped to the subcarrier indices rather than to the transmit AEs of the SM [16] or the generalized SM (GSM) [39], an adaptive SIM-OFDM may also be conceived. Specifically, in contrast to the classic SIM-OFDM system, where equal-length subcarrier index bit-segments are mapped to the
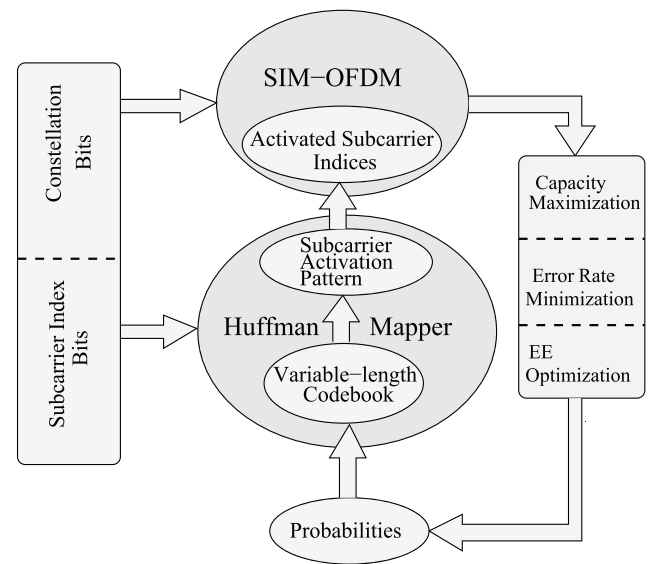

FIGURE 1. The conceptual framework illustrating the employment of Huffman mapping based variable-length codebook for the selection of the subcarrier indices of the SIM-OFDM scheme. The probabilities associated with the Huffman coding are gleaned from the optimization of the capacity, the error performance as well as the energy-efficiency of the system.

subcarriers activated, the subcarrier activation pattern may be adaptively selected by using the variable-length coding strategy of Huffman codes [37]. In this paper, we propose an adaptive SIM-OFDM scheme relying on the variable-length entropy coding technique of Huffman codes [37], which is usually used for the lossless compression of source information. The proposed conceptual framework is shown in Fig. 1. The index bits of the classic SIM-OFDM system are mapped equi-probably to the subcarriers activated. By contrast, channel-aware and energy-aware probabilities of the different subcarrier activation patterns may be obtained by optimizing either the channel-capacity or the error-rate and/or the energy-efficiency (EE) of the system. Using these probabilities, the Huffman mapper of Fig. 1 is capable of generating variable-length codebooks. The subcarrier index bits may be mapped to the corresponding subcarrier activation patterns of the SIM-OFDM system.

It is noteworthy at this point that since the codewords generated by the Huffman mapper are of variable length, the mapped SIM-OFDM frames will be constituted of variable number of source bits. Some of the subcarrier activation patterns of the classic SIM-OFDM system were unutilized. The reason for this inefficiency is that if the number of combinations of activating N_p subcarriers from a total number of N_c subcarriers is not a power of 2, then at best $\left\lfloor \log_2 \binom{N_c}{N_p} \right\rfloor$ bits can be mapped to the subcarriers activated. This is equally true for the generalized SM scheme of [39] and for the generalized space-time shift keying (GSTSK) scheme of [40]. By contrast, our proposed Huffman coding based adaptive SIM-OFDM scheme has the potential of exploiting all the legitimate $\binom{N_c}{N_p}$ subcarrier activation patterns, which is

an explicit benefit of the variable-length codebook utilized. This has the additional advantage that the decoding of the proposed system does not get trapped in the 'catastrophic set of active indices', as eloquently mentioned in [7].

The contributions of this paper may thus be summarized as follows:

1) We conceive a Huffman coding based adaptive SIM-OFDM technique for dispersive channels and characterize the capacity, bit-error-ratio (BER) and EE of the system. Furthermore, we devise the procedure of adaptively selecting the subcarriers activated relying on the Huffman coding principle.

2) While the conventional SIM-OFDM system of [7], [9], and [13] can only activate $2^{\left\lfloor \log_2 \binom{N_c}{N_p} \right\rfloor}$ subcarrier activation patterns, the proposed system is capable of activating all the $\binom{N_c}{N_p}$ legitimate patterns of subcarriers.

3) The system relies on the ML detector proposed or on the reduced-complexity log-likelihood (LLR)-based detector using the philosophy of [7]. However, since the system exploits all the legitimate subcarrier activation patterns, our new system has the additional advantage that in contrast to [7], it does not mistakenly detect any of the unutilized set of subcarriers.

4) Furthermore, since the subcarrier activation strategy is dependent on a number of probabilities gleaned from an optimization procedure, the proposed system is capable of adaptively striking a beneficial compromise amongst the capacity, the error performance as well as EE of the system.

A. OUTLINE

The organization of the paper is as follows. In Section II, we provide an overview of our adaptive SIM-OFDM system and detail its transceiver architecture. The subcarrier mapping of the scheme relying on variable-length Huffman coding is described in Section III. Striking a tradeoff amongst the attainable capacity, the error performance and EE of our entropy-coded SIM-OFDM system is elaborated on in Section IV. Section V provides our numerical results demonstrating the efficacy of the proposed scheme. Finally, we conclude in Section VI.

B. NOTATIONS

The following notations are employed in this paper. We use capital boldface letter for example A, boldface lowercase letter a and the notation A: to represent a matrix, a vector and a block matrix respectively. The notations A^T, A^H, $\text{tr}(A)$, $\text{vec}(A)$, $|A|$ and $\|A\|$ represent the matrix transpose, the Hermitian transpose, the trace, the vectorial stacking operator, the determinant and the Frobenius norm of A, respectively. The operator $\otimes$ represents the Kronecker product, $\mathcal{E}\{\bullet\}$ the expected value of '$\bullet$', I_T the $(T \times T)$-element identity matrix and $0_{M \times T}$ the $(M \times T)$−element zero matrix. The notation `diag`$\{x_1, \ldots, x_N\}$ denotes a diagonal matrix with $x_1, \ldots, x_N$ on its main diagonal, $\Pr(\cdot)$ the probability

of '·', while the N_c−point DFT of the symbol stream '•' and the N_c−point inverse DFT (IDFT) of '•' are denoted by $\text{DFT}_{N_c}\{\bullet\}$ and $\text{IDFT}_{N_c}\{\bullet\}$, respectively. The corresponding DFT and the IDFT matrices are represented by $\mathcal{F}_{N_c}$ and $\mathcal{F}_{N_c}^H$, respectively. Furthermore, $\mathcal{CN}(\mu, \sigma^2)$ refers to the circularly symmetric complex Gaussian distribution with a mean of μ and a variance of σ^2.

II. SYSTEM OVERVIEW OF THE ADAPTIVE SIM-OFDM

Fig. 2 shows the schematic of our proposed adaptive SIM-OFDM system communicating over frequency-selective Rayleigh fading channels. Furthermore, N_c subcarriers are employed by our OFDM modem, out of which N_p subcarriers are utilized by the SIM-OFDM for the transmission of the codeword symbols and the remaining subcarriers are *not activated*, i.e. they do not carry classic modulated symbols.

A. THE TRANSMITTER MODEL

Let us consider b source bits, which are to be transmitted in parallel during an OFDM symbol interval employing a total of N_c parallel subcarriers, as shown in Fig. 2. The b bits are partitioned into b_1 and b_2 bits. The b_1 bits are mapped to the classic $\mathcal{L}$-PSK/QAM symbols. By contrast, the b_2 bits are used for selecting the indices of the subcarriers of the SIM-OFDM scheme, respectively and may be termed as the 'index bits'. Each of these bits are further partitioned into K parallel blocks. We use a single $\mathcal{L}$-PSK/QAM constellation, hence each of the K parallel blocks and each of the N_a symbols in a particular parallel block contains an equal number of bits. By contrast, the number of index bits varies owing to using Huffman coding. Furthermore, the total number N_c of the available subcarriers is divided into N_b subcarriers for each of the K parallel blocks, where $N_c = KN_b$. Similarly, the total of N_p subcarriers to be selected by the SIM scheme is also partitioned into K blocks of N_a subcarriers each, where we have $N_p = KN_a$. The N_a number of symbols generated may be expressed by,

$$S^k = \left(S^k[1], S^k[2], \ldots, S^k[N_a]\right)^T. \quad (1)$$

The b_2 bits of Fig. 2 are mapped to the appropriate variable-length codewords of the Huffman codebook in order to select the index to the N_a subcarriers activated from the N_b subcarriers for each block. As shown in Fig. 2, the b_2 bits are separated into K subblocks depending on the lengths of the codewords output by the Huffman codebook, so that each of the K subblocks activates a $(N_a \times 1)$−element subcarrier activation vector a^k:

$$a^k = \left(a^k[1], a^k[2], \ldots, a^k[N_a]\right)^T, \quad (2)$$

where $a^k[n_a]$ $(n_a = 1, 2, \ldots, N_a)$ represents the index of the n_a−th subcarrier activated in a particular OFDM symbol duration.

Following the bit mapping to classic constellation symbols and the activation of the subcarriers represented by the vector of indices a^k $(k = 1, 2 \ldots, K)$, the symbols of all the
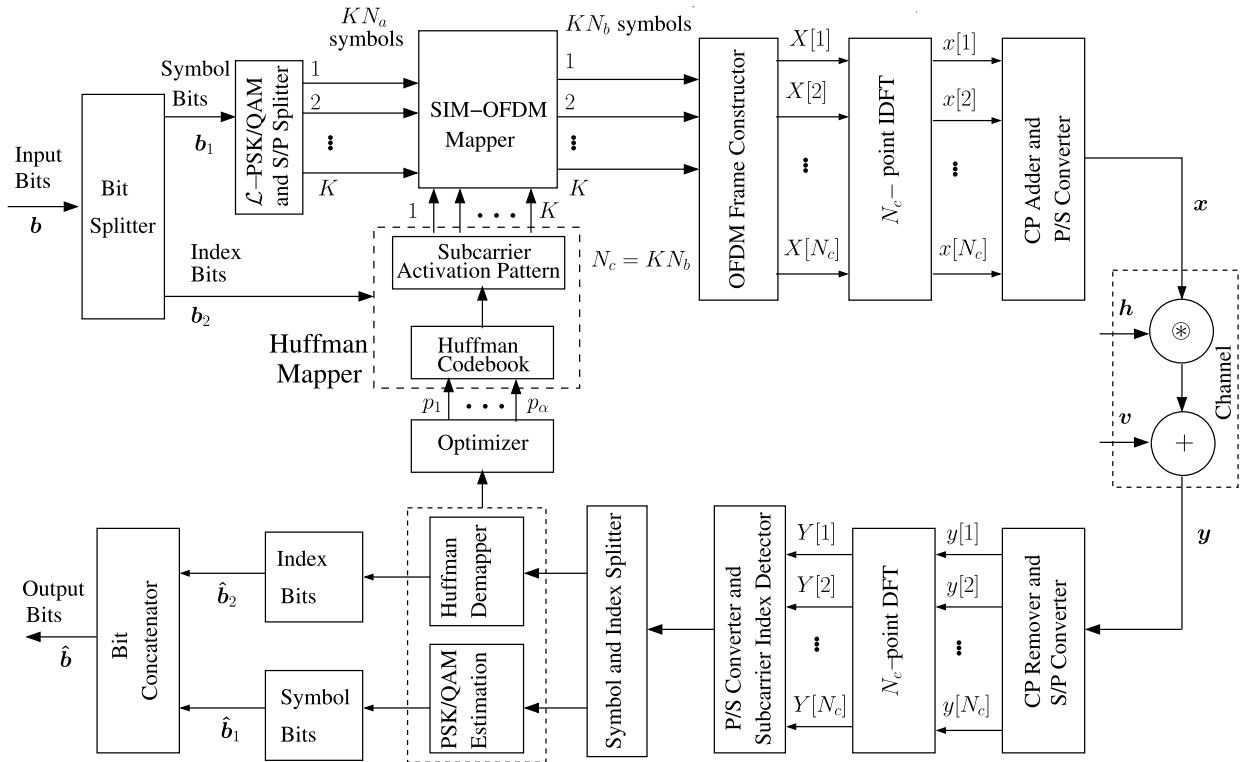
FIGURE 2. Schematic diagram of the proposed adaptive SIM-OFDM transceiver relying on Huffman coding principle. A total of $N_c = KN_a$ symbols along with the subcarrier indices mapped by Huffman coding are passed through the SIM-OFDM mapper and the symbols are appropriately mapped to N_c subcarriers for transmission over dispersive channel.

K subblocks are concatenated to form OFDM frames and are transmitted after appropriate OFDM processing. To be more specific, the N_a symbols defined by $S^k[1], S^k[2], \ldots, S^k[N_a]$ along with the subcarrier activation pattern $\boldsymbol{a}^k$ for each of the parallel subblocks $k = 1, 2 \ldots K$ are passed through the 'OFDM Frame Constructor' block of Fig. 2, which generates a total of N_c frequency-domain (FD) symbols $X[1], X[2], \ldots, X[N_c]$. In contrast to the classic OFDM, however, not all the N_c terms of the resultant OFDM symbol denoted by the vector $\boldsymbol{X}$ contain constellation symbols. Rather, a total of $N_p = KN_a$ symbols are assigned to N_p subcarriers in each OFDM frame, whereas the remaining $(N_c - N_p) = k(N_b - N_a)$ subcarriers are 'inactive', i.e. blank.

To be more specific, assuming the relationship $N_c = KN_b$, a number of N_b subcarriers are utilized per parallel block. Due to the basic philosophy of the SIM scheme, N_a subcarriers out of the N_b subcarriers per block are activated and are modulated by the FD codeword symbols $S^k[1], S^k[2], \ldots, S^k[N_a]$ $k = 1, 2 \ldots K$ employing the subcarrier selection pattern $\boldsymbol{a}^k$. The 'OFDM Frame Constructor' generates N_b FD symbols represented by $X^k[1], X^k[2], \ldots, X^k[N_b]$ $k = 1, 2, \ldots, K$ for each block and the K parallel blocks thus generate a total of N_c FD symbols $\boldsymbol{X} = (X[1], X[2], \ldots, X[N_c])^T$, which constitute an OFDM symbol. Upon denoting the N_c−point DFT matrix

and the IDFT matrix by $\mathcal{F}_{N_c}$ and $\mathcal{F}_{N_c}^H$ respectively, we have the time-domain (TD) samples given by [9], [41], [42]:

$$\boldsymbol{x} = \sqrt{\frac{N_c}{N_p}} \text{IDFT}_{N_c}\{X\} = \sqrt{\frac{N_c}{N_p}} \mathcal{F}_{N_c}^H \boldsymbol{X}. \quad (3)$$

The corresponding SIM-OFDM scheme may be unambiguously described by the (N_c, N_p, K) parameters.

B. THE SUBCARRIER MAPPING

Consider the formation of the OFDM frame, as discussed in Section II-A above. The FD symbols $\boldsymbol{X}^k = X^k[1], X^k[2], \ldots, X^k[N_b]$ for a particular block k may be viewed as:

$$\boldsymbol{X}^k = \underbrace{\left(S^k[1], 0, 0, S^k[2], \ldots, 0, S^k[N_a]\right)^T}_{N_a \text{ out of } N_b \text{ elements are nonzero}}, \quad (4)$$

where $\boldsymbol{S}^k = \{S^k[1], S^k[2], \ldots, S^k[N_a]\}$ represents the N_a constellation symbols given by (1). Eq. (4) may be further expressed as [38]:

$$\boldsymbol{X}^k = \boldsymbol{a}^k \cdot \boldsymbol{S}^k, \quad (5)$$

where $\boldsymbol{a}^k$ belongs to a finite set of $\alpha = \binom{N_b}{N_a}$ subcarrier activation patterns given by

$$\mathcal{A}^k = \{\boldsymbol{a}_1^k, \boldsymbol{a}_2^k, \ldots, \boldsymbol{a}_\alpha^k\}, \quad (6)$$

while a_i^k is the i-th ($N_a \times 1$)−element subcarrier activation vector as given by (2). When a_i^k is selected, the N_a subcarriers corresponding to it are activated and the remaining ($N_b - N_a$) are inactive.

We denote the probability of selecting the i-th subcarrier activation pattern by $p_i = \Pr\left(a^k = a_i^k\right)$, so that we have $\sum_{i=1}^{\alpha} p_i = 1$.

Note that in the conventional SIM-OFDM of [7], [9], and [13], the index bits are mapped equi-probably to the subcarrier activation patterns, i.e. the probabilities of selecting the different subcarrier activation patterns are equal, which is given by:

$$\mathfrak{p} = \{p_1, p_2, \dots, p_\alpha\}$$
$$= \left\{\frac{1}{\alpha}, \frac{1}{\alpha}, \dots, \frac{1}{\alpha}\right\}. \tag{7}$$

By contrast, the probabilities in our proposed adaptive SIM-OFDM system are not equal. They are dependent on the channel quality and are obtained by employing an optimization procedure in order to maximize the channel capacity and/or EE under the requirement of a specific bit/symbol error ratio performance. Depending on the values of the probabilities, the Huffman mapper constructs a variable-length codebook. The Huffman codebook is used for mapping the incoming index bits to the subset of subcarriers activated.

C. THE RECEIVER MODEL

Let us assume the channel to be frequency-selective, whose discrete-time channel impulse respone (CIR) is given by h. Assuming perfect synchronization, the discrete-time signal at the receiver can be expressed by [30]

$$y = h \circledast x + \mathbf{v}, \tag{8}$$

where $\circledast$ denotes the N_c-point circular convolution operator and $\mathbf{v}$ represents the corresponding time-domain (TD) additive white Gaussian noise (AWGN). After removing the CP, the received signal is first demodulated by applying the N_c-point discrete Fourier transform (DFT). The resultant FD output $Y = (Y[1], Y[2], \dots, Y[N_c])^T \in \mathbb{C}^{N_c \times 1}$ may be written as [30]:

$$Y = \mathcal{F}_{N_c} y$$
$$= \mathcal{F}_{N_c} (h \circledast x + \mathbf{v})$$
$$= \tilde{H}X + V, \tag{9}$$

where $\tilde{H} = \text{diag}\{\tilde{H}[1], \tilde{H}[2], \dots, \tilde{H}[N_c]\} \in \mathbb{C}^{N_c \times N_c}$ is a diagonal matrix whose diagonal elements are obtained by $\mathcal{F}_{N_c} h \in \mathbb{C}^{N_c \times 1}$ representing the FD channel transfer functions. Still referring to ((9)), we have the FD signal $X = (X[1], X[2], \dots, X[N_c])^T \in \mathbb{C}^{N_c \times 1}$ and the FD AWGN $V = \mathcal{F}_{N_c} \mathbf{v} \in \mathbb{C}^{N_c \times 1}$ having a zero mean and a variance of N_0.

After the N_c-point DFT processing, the receiver detects the bits mapped to the constellation symbols as well as those mapped to the subcarrier indices. Due to the variable-length nature of the Huffman coding based index bits, conceiving a joint detector for simultaneously detecting both types of bits is not feasible. As shown in Fig. 2, the activated subcarriers are detected first. From the subcarrier activation pattern, the index bits may be detected using Huffman demapping and the constellation symbols may then be readily detected by a maximmum-likelihood (ML) detector.

1) ML DETECTOR

As mentioned above, an ML detector may only be used in conjunction with our scheme after detecting the subcarriers activated. This may be performed by another ML search over all the OFDM subcarriers. In this search, a zero symbol is considered along with the $\mathcal{L}$ legitimate PSK/QAM symbols. If the detector detects zero rather than any of the $\mathcal{L}$ PSK/QAM symbols, then that subcarrier is considered to be inactive.

To be specific, the ML detector may be formulated as follows:

$$\hat{s}_l = \arg \min_{s_l \in \mathbb{S}} \left\| Y[n_c] - \tilde{H}[n_c] X[n_c] \right\|^2, \quad n_c = 1, 2, \dots, N_c \tag{10}$$

where the set $\mathbb{S}$ consists of all the $\mathcal{L}$ PSK/QAM symbols, s_l, $l = 1, 2, \dots, \mathcal{L}$ and a zero symbol. After detecting the subcarriers activated, the ML detector then detects the $\mathcal{L}-$ PSK/QAM symbols, which does not include the search over the zero symbol. The detected subcarrier patterns are then utilized for detecting the index bits with the aid of the Huffman demapper of Fig. 2.

2) REDUCED-COMPLEXITY SOFT-DECISION DETECTOR

To avoid the high computational complexity of the ML detector of (10), we further propose a soft-decision detector based on (9) by relying on the logarithmic likelihood ratio (LLR) of the FD symbol. Additionally, since all the potential combinations of selecting N_a subcarriers out of the N_b available subcarriers can be used in our proposed scheme with the aid of variable-length coding, this detector does not detect any of the unutilized subcarriers patterns in contrast to [7], [9], and [13]. According to the SIM-OFDM signalling strategy, some of the FD symbols are either non-zeros or zeros depending on whether the corresponding subcarriers are activated or de-activated. We thus define the LLR [7], [43] $L(n_c)$ of the n_c−th symbol in terms of the ratio of the following *a posteriori* probablities,

$$L(n_c) \triangleq \ln \frac{\sum_{\mu=1}^{\mathcal{L}} \Pr(X[n_c] = s_l \mid Y[n_c])}{\Pr(X[n_c] = 0 \mid Y[n_c])}. \tag{11}$$

Note that $\sum_{\mu=1}^{\mathcal{L}} \Pr(X[n_c] = s_l) = \frac{N_p}{N_c}$ and $\Pr(X[n_c] = 0) = \frac{(N_c - N_p)}{N_c}$. Using Bayes theorem in (11), we obtain [7], [44]:

$$
L(n_c) = \ln(N_p) - \ln(N_c - N_p) + \frac{\|Y[n_c]\|^2}{2N_0}
$$
$$
+ \ln\left(\sum_{\mu=1}^{\mathcal{L}} \exp\left(-\frac{1}{2N_0}\left\|Y[n_c] - \tilde{H}[n_c]X[n_c]\right\|^2\right)\right).
$$
(12)

For the sake of reducing the computational burden of the maximum *a posteriori* (MAP) algorithm, the Jacobian logarithm-based approximate logarithmic MAP (approx-log-MAP) algorithm [45] may be invoked in (12). Specifically, using $N_p = N_c/2$, we have from (12):

$$
L(n_c) = \frac{\|Y[n_c]\|^2}{2N_0} + \text{jac}\left(\sum_{\mu=1}^{\mathcal{L}} \exp\left(-\frac{1}{2N_0}\|Y[n_c]\right.\right.
$$
$$
\left.\left. -\tilde{H}[n_c]X[n_c]\right\|^2\right)\right), \quad (13)
$$

where jac ($\bullet$) represents the Jacobian logarithm of '$\bullet$', which is recursively computed [45] over the $\mathcal{L}$ terms using

$$
\text{jac}\left(\sum_{i=1}^{2} \exp(\delta_i)\right) = \max(\delta_1, \delta_2) +
$$
$$
\ln(1 + \exp(-|\delta_1 - \delta_2|)).
$$

After calculating the LLRs corresponding to all the N_c subcarrier symbols, the detector then detects the N_p subcarriers activated. The detector decides in favour of the highest N_p LLR values and the corresponding subcarriers are deemed to be activated and the subcarrier index bits are estimated by the Huffman demapper of Fig. 2. After estimating the subcarrier index bits, the estimation of the bits mapped to $\mathcal{L}-$ PSK/QAM symbols is straight-forward. This may performed using the ML detector

$$
\hat{s}_l = \arg\min_{s_l}\left\|Y[n_c] - \tilde{H}[n_c]X[n_c]\right\|^2, \quad n_c = 1, 2, \ldots, N_c
$$
(14)

where the ML search is carried out only over the constellation symbols.

A close look into the two above-mentioned detectors reveals that the LLR-based detector is capable of detecting the source information with almost the same integrity as the ML detector, while it imposes a significantly reduced decoding complexity. For all of the $\alpha = \binom{N_b}{N_a}$ subcarrier activation patterns corresponding to any of the K parallel subblocks, the ML detector has to simultaneously detect N_a subcarrier symbols having a search space of $\mathcal{L}^{N_a}$ constellation symbols. As a result, the ML detector imposes a decoding complexity of $\mathcal{O}(\alpha \mathcal{L}^{N_a})$ per parallel block in terms of the number

of complex-valued multiplications, which may render the detector impractical, especially in the case of large values of α and N_a. By contrast, the soft detector imposes a modest complexity of $\mathcal{O}(\mathcal{L})$ per subcarrier in terms of the number of complex multiplications required for calculating the LLRs given by (12) and the subsequent symbol detection using (14), which can again be reduced either by using the log-max-MAP [45] or the Jacobian-based log-approx-MAP technique given by (13). Note furthermore from the LLR definition of (11) that the logarithm of the sum of the probabilties of the constellation symbols compared to the null symbol is taken into account in calculating the LLRs. As a result, the LLR values are significantly higher for the subcarriers activated compared to the inactive subcarriers, which beneficially assists the LLR detector in detecting the subcarrier activation patterns and thereby the index bits. Consequently, the LLR detector is capable of exhibiting a near-optimal performance, despite the fact that the decoding complexity is significantly reduced. Additionally, as a benefit of employing the variable-length Huffman codebook, all the subcarrier activation patterns can be used and there is no possibility that our LLR detector will catastrophically detect an unused subcarrier pattern, which is possible for the LLR detector of [7].

III. HUFFMAN CODING TECHNIQUE FOR ADAPTIVE SIM-OFDM

As already mentioned above, Huffman coding based variable-length codewords are employed in our SIM-OFDM scheme for selecting the appropriate subcarrier activation pattern. In this section, we illustrate the Huffman coding aided subcarrier activation procedure.

Huffman coding is an entropy coding scheme which has been predominantly employed for lossless data compression. It exploits the probability of occurrence of a source symbol for mapping the high-probability symbols to a low number of bits and vice versa. We design our codebook for mapping the subcarrier index bits depending on some probabilities obtained from the optimization of either the capacity or the EE of the system. Again, subcarrier patterns with higher probability are mapped to a smaller number of index bits, whereas those with lower probability are mapped to a higher number of index bits. In addition, no codeword in the codebook should be the prefix to any of the other codewords. Huffman codes are generated by creating a binary tree of nodes. The procedure begins by sorting the symbols in ascending order of their probabilities or frequencies [37]. While there are more than two nodes, the two nodes having the lowest probabilities are removed and a new node relying on these two nodes and with a probability equal to the sum of the two nodes' probabilities is created. The nodes are then sorted again and the process continues [37]. The codes for any of the symbols are assigned by traversing the tree from the root and assigning a 0 for a higher probabilty node and a 1 for a lower probabilty node. The process is illustrated by following the example of Fig. 3 and Fig. 4 for an $(N_b = 4, N_a = 2, K = 16)$
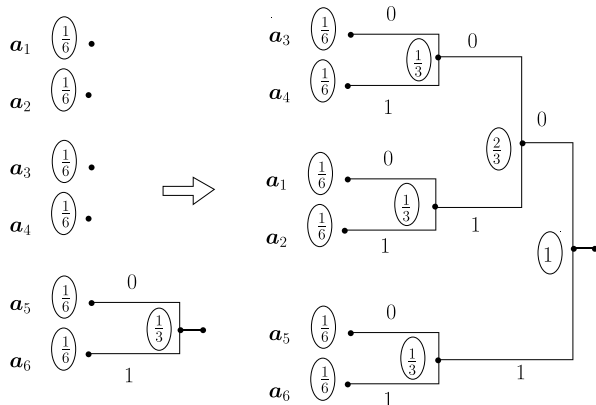
FIGURE 3. Huffman mapping for probabilities, $\mathbb{p} = \left\{\frac{1}{6}, \frac{1}{6}, \frac{1}{6}, \frac{1}{6}, \frac{1}{6}, \frac{1}{6}\right\}$. Only the first and the last steps of the Huffman mapping procedure are shown [37].
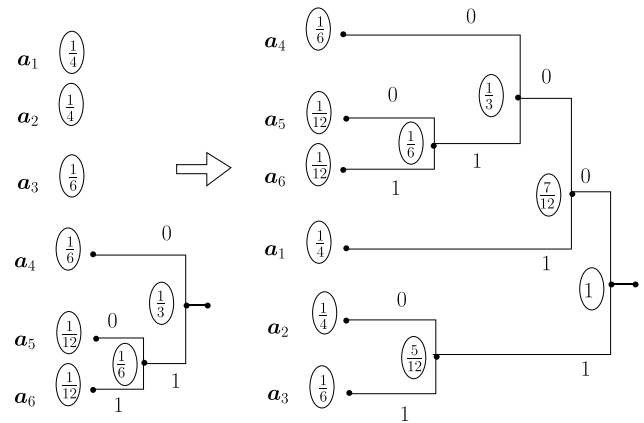

FIGURE 4. Huffman mapping example corresponding to the typical set of probabilities, $\mathbb{p} = \left\{\frac{1}{4}, \frac{1}{4}, \frac{1}{6}, \frac{1}{6}, \frac{1}{12}, \frac{1}{12}\right\}$. Only the first and the last steps are shown [37].

SIM-OFDM system with two sets probabilities for the legitimate subcarrier activation patterns. In Fig. 3 and Fig. 4, only the first and the last steps of the Huffman coding procedure are shown for space economy.

Example: Let us now exemplify the subcarrier-allocation strategy of our SIM-OFDM considering $N_c = 64$, $N_p = 32$ and $K = 16$, which gives us $N_b = 4$, $N_a = 2$.

The conventional subcarrier mapping of [6], [7], and [9] for these parameter values may be expressed by the (6×4) −element binary matrix

$$A_{6,4}^k = \begin{bmatrix} 1 & 1 & 0 & 0 \\ 1 & 0 & 1 & 0 \\ 1 & 0 & 0 & 1 \\ 0 & 1 & 1 & 0 \\ 0 & 1 & 0 & 1 \\ 0 & 0 & 1 & 1 \end{bmatrix} \in \mathbb{Z}^{6\times 4}. \qquad (15)$$

Specifically, the 6 rows of the matrix represent the 6 potential candidates of the subcarrier activation pattern and the location of the 1's in each row indicates the subcarriers activated. Thus the six legitimate subcarrier patterns of the conventional systems are: $a_1^k = (1,2)^T$, $a_2^k = (1,3)^T$, $a_3^k = (1,4)^T$, $a_4^k = (2,3)^T$, $a_5^k = (2,4)^T$ and $a_6^k = (3,4)^T$. The $b_2 = \left\lfloor \log_2\binom{4}{2} \right\rfloor = 2$ bits may, however, be mapped to $2^2 = 4$ rows of the binary matrix and the last 2 of the 6 rows are discarded. The conventional system thus uses the 4 activation patterns $a_1^k = (1,2)^T$, $a_2^k = (1,3)^T$, $a_3^k = (1,4)^T$ and $a_4^k = (2,3)^T$ only.

By contrast, our proposed SIM-OFDM scheme exploits all the 6 subcarrier activation patterns and employs a Huffman coding based approach rather than using the equi-probable binary matrix $A_{6,4}^k$ of (15). We exploit the probabilities p_i $i = 1, 2, \ldots, \alpha$ for all the legitimate $\alpha = \binom{N_b}{N_a} = 6$ subcarrier activation patterns. For the sake of exemplifying our mapping procedure, we consider two sets of probabilities $\mathbb{p} = \left\{\frac{1}{6}, \frac{1}{6}, \frac{1}{6}, \frac{1}{6}, \frac{1}{6}, \frac{1}{6}\right\}$ and $\mathbb{p} = \left\{\frac{1}{4}, \frac{1}{4}, \frac{1}{6}, \frac{1}{6}, \frac{1}{12}, \frac{1}{12}\right\}$ here. The corresponding Huffman coding tree is shown in

TABLE 1. Huffman mapping of codeword bits to subcarrier activation patterns for $\mathbb{p} = \left\{\frac{1}{6}, \frac{1}{6}, \frac{1}{6}, \frac{1}{6}, \frac{1}{6}, \frac{1}{6}\right\}$.

Codeword Bit Sequence	Probability, p_i	Subcarrier Activation Pattern, a_i
010	$\frac{1}{6}$	$a_1 = (1,2)^T$
011	$\frac{1}{6}$	$a_2 = (1,3)^T$
000	$\frac{1}{6}$	$a_3 = (1,4)^T$
001	$\frac{1}{6}$	$a_4 = (2,3)^T$
10	$\frac{1}{6}$	$a_5 = (2,4)^T$
11	$\frac{1}{6}$	$a_6 = (3,4)^T$

Fig. 3 and Fig. 4, respectively. The encoding process is performed by assigning a 0 for the node with higher probability and a 1 for that with a lower probabilty. The mapping of the codewords to the corresponding subcarrier activation patterns are shown in Table 1 and Table 2. Note that we have shown only the first and the last steps for the generation of the Huffman tree [37] in Fig. 3 and Fig. 4. The subscript k of a_i^k is not shown in Fig. 3 and Fig. 4 and either in Table 1 or in Table 2 for the sake of notational simplicity.

It is worth noting at this point that the probability values for the different subcarrier patterns are obtained by an optimization procedure. The Huffman mapper of Fig. 2 maps the random index bitstream of the source information to the appropriate subcarrier activation patterns. This mapping relies on the probability values depending on the channel conditions. The channel state information assists in optimizing either the capacity or the error performance and/or the EE of the system and this optimization provides the unequal probability values. Using the probability values, the Huffman mapper of Fig. 2 generates the variable-length Huffman codebook. The incoming random index bitstream is mapped to the OFDM subcarriers activated using the Huffman codebook generated.

TABLE 2. Huffman mapping of codeword bits to subcarrier activation patterns for $\mathfrak{p} = \left\{ \frac{1}{4}, \frac{1}{4}, \frac{1}{6}, \frac{1}{6}, \frac{1}{12}, \frac{1}{12} \right\}$.

Codeword Bit Sequence	Probability, p_i	Subcarrier Activation Pattern, $\boldsymbol{a}_i$
01	$\frac{1}{4}$	$\boldsymbol{a}_1 = (1,2)^T$
10	$\frac{1}{4}$	$\boldsymbol{a}_2 = (1,3)^T$
11	$\frac{1}{6}$	$\boldsymbol{a}_3 = (1,4)^T$
000	$\frac{1}{6}$	$\boldsymbol{a}_4 = (2,3)^T$
0010	$\frac{1}{12}$	$\boldsymbol{a}_5 = (2,4)^T$
0011	$\frac{1}{12}$	$\boldsymbol{a}_6 = (3,4)^T$

Since the Huffman codebook is of variable length, the index bits mapped to different subcarrier activation patterns are not equal in number.

The Huffman codebook has the unique property that no codeword is a prefix of any other codeword. As a result, the incoming subcarrier index bits can be uniquely mapped to the subcarrier activation patterns. Moreover, the bijective function of Table 1 between the codewords and the subcarrier patterns facilitates unambiguous decoding of the mapping patterns to the index bits transmitted. To be more specific, the incoming index bits b_2 of Fig. 2 are sequentially and uniquely mapped to the subcarrier activation patterns $\boldsymbol{a}_i^k$. As shown in Table 1 for the probabilities $\mathfrak{p} = \left\{ \frac{1}{6}, \frac{1}{6}, \frac{1}{6}, \frac{1}{6}, \frac{1}{6}, \frac{1}{6} \right\}$, if the incoming bit 1 is followed by another 1, then the subcarriers 3 and 4 (corresponding to pattern $\boldsymbol{a}_6^k = (3,4)^T$) are activated for the parallel block k. However, if the first 1 is followed by a 0, then the subcarriers 2 and 4 (corresponding to pattern $\boldsymbol{a}_5^k = (2,4)^T$) are activated for the $k-$th subblock. Similarly, for the first incoming bit of 0, there are 4 different patterns of activating the subcarriers. Bearing in mind the variable length of the bit-pattern to be mapped to the subcarriers, the average number of index bits per subcarrier activation pattern may be computed as $\frac{1}{6} \times 2 + \frac{1}{6} \times 2 + \frac{1}{6} \times 4 + \frac{1}{6} \times 4 + \frac{1}{6} \times 4 + \frac{1}{6} \times 4 = 2.67$ bits.

On the other hand, when the probabilities are $\mathfrak{p} = \left\{ \frac{1}{4}, \frac{1}{4}, \frac{1}{6}, \frac{1}{6}, \frac{1}{12}, \frac{1}{12} \right\}$, the mapping of the incoming bits b_2 of Fig. 2 is shown in Table 2. Due to the unique prefix property of Huffman coding, all the potential incoming bit combinations are included in Table 2, where the bit sequences are unambiguously mapped to the subcarrier activation patterns $\boldsymbol{a}_1^k = (1,2)^T$, $\boldsymbol{a}_2^k = (1,3)^T$, $\boldsymbol{a}_3^k = (1,4)^T$, $\boldsymbol{a}_4^k = (2,3)^T$, $\boldsymbol{a}_5^k = (2,4)^T$ and $\boldsymbol{a}_6^k = (3,4)^T$ during the $k-$th subblock duration. Since there is a one-to-one correspondence between the codeword bit sequences and the subcarrier activation patterns, the subcarriers activated for subblock k can be uniquely decoded to the subcarrier index bits. Table 2 illustrates the variable-length codewords mapped to subcarriers activated for probabilities $\mathfrak{p} = \left\{ \frac{1}{4}, \frac{1}{4}, \frac{1}{6}, \frac{1}{6}, \frac{1}{12}, \frac{1}{12} \right\}$. Under these probability values, the average number of bits

transmitted via the subcarrier indices are $\frac{1}{4} \times 2 + \frac{1}{4} \times 2 + \frac{1}{6} \times 2 + \frac{1}{6} \times 3 + \frac{1}{12} \times 4 + \frac{1}{12} \times 4 = 2.50$ bits.

The proposed adaptive SIM-OFDM system finds the set of probabilities $\mathfrak{p}$ in order to optimize its performance. The optimization problem may be formulated as

$$\max_{\mathfrak{p}} / \min F(\mathfrak{p})$$
$$\text{s.t. } \mathfrak{p} \in \mathbb{P} \qquad (16)$$

where $F(\mathfrak{p})$ is the objective function (OF) dependent on the probabilities $\mathfrak{p}$ and $\mathbb{P}$ is the legitimate domain of $\mathfrak{p}$. Considering the binary nature of the bit mapping as well as of the Huffman coding tree and the number of combinations available for activating N_a out of N_b subcarriers, we consider the following discrete set as the domain of $\mathfrak{p}$:

$$\mathbb{P} = \left\{ \mathfrak{p} \mid \sum_{i=1}^{\alpha} p_i = 1, \quad p_i = 0, 1, 2^{-1}, 2^{-2}, \cdots, 2^{-\beta}, \right. \\ \left. \alpha^{-1}, (2\alpha)^{-1}, \cdots, (2\alpha)^{-\beta} \right\}, \qquad (17)$$

where β is the probability search depth and $1 \leq \beta \leq N_b$.

IV. CAPACITY-OPTIMAL, SYMBOL ERROR RATE (SER-) OPTIMAL AND EE-OPTIMAL ADAPTIVE SIM-OFDM

In this secttion, we propose the capacity-optimal, the SER-optimal and the EE-optimal design of our adaptive SIM-OFDM system. Specifically, we optimize our system for maximizing the OF of capacity, SER as well as EE for finding the best set of probabilities, $\mathfrak{p}$.

A. CAPACITY-OPTIMAL DESIGN

In this approach, our objective is to find $\mathfrak{p}$, which maximizes the capacity of our adaptive SIM-OFDM system. The problem is formulated as:

$$\max_{\mathfrak{p}} C(\mathfrak{p})$$
$$\text{s.t. } \mathfrak{p} \in \mathbb{P}. \qquad (18)$$

Consider the system model given by (9). When the subcarrier activation pattern $\boldsymbol{a}_i^k$ is encountered in the $k-$th subblock, the received signal corresponding to the $k-$th subblock may be expressed by

$$\boldsymbol{Y}_i^k = \tilde{\boldsymbol{H}}_i^k \boldsymbol{X}_i^k + \boldsymbol{V}_i^k, \qquad (19)$$

where

$$\boldsymbol{Y}_i^k = \boldsymbol{Y}^k \mid \left(\boldsymbol{a}^k = \boldsymbol{a}_i^k \right) \in \mathbb{C}^{N_b \times 1}, \qquad (20)$$

$$\tilde{\boldsymbol{H}}_i^k = \text{diag}\{\tilde{H}[1], \tilde{H}[2], \ldots, \tilde{H}[N_b]\}$$

$$= \underbrace{\begin{bmatrix} \tilde{H}[1] & 0 & 0 & 0 \\ 0 & \tilde{H}[1] & 0 & 0 \\ 0 & 0 & \ddots & 0 \\ 0 & 0 & 0 & \tilde{H}[N_b] \end{bmatrix}}_{N_a \text{ out of } N_b \text{ diagonal elements are nonzero}} \in \mathbb{C}^{N_b \times N_b} \qquad (21)$$

and

$$X_i^k = \begin{bmatrix} S^k[1] \\ 0 \\ S^k[2] \\ 0 \\ \vdots \\ S^k[N_a] \end{bmatrix} \mid \left(a^k = a_i^k \right) \in \mathbb{C}^{N_b \times 1}. \qquad (22)$$

$$\underbrace{}_{\substack{N_a \text{ out of} \\ N_b \text{ elements} \\ \text{are nonzero}}}$$

For the sake of notational simplicity, we denote the conditional probability density function (PDF) $f\left(Y^k \mid a^k = a_i^k\right) \ \forall k$ by $f_i(Y)$, and we have, $f(Y) = \sum_{i=1}^{\alpha} p_i f_i(Y)$.

The capacity of the scheme may be expressed in terms of the mutual information $I(X; Y)$ in a manner similar to [18]

$$C = W(C_1 + C_2), \qquad (23)$$

where W denotes the subcarrier bandwidth and $C_1 = I\left(X^k; Y^k \mid a^k\right) \ \forall k$ represents the amount of information transmitted using the $\mathcal{L}-$PSK/QAM symbols, whereas $C_2 = I\left(a^k; Y^k\right) \ \forall k$ denotes the information mapped to the specific indices of the subcarries activated.

Furthermore, denoting the signal-to-noise ratio (SNR) by $\gamma = \frac{\sigma_X^2}{N_0}$, where σ_X^2 is the transmit signal power of each of the subcarriers, C_1 and C_2 may be expressed [18], [38], [46] by

$$C_1 = I\left(X^k; Y^k \mid a^k\right) = \sum_{i=1}^{\alpha} p_i \log_2\left(1 + \gamma \sum_{k=1}^{K} \|\tilde{H}_i^k\|^2\right) \qquad (24)$$

and

$$C_2 = I\left(a^k; Y^k\right) = \sum_{i=1}^{\alpha} p_i \int_Y f_i(Y) \log_2 \frac{f_i(Y)}{f(Y)} dY. \qquad (25)$$

It is difficult to further simplify (25) to obtain a closed-form expression. However, both the upper and the lower bound of C_2 may be found similarly to [18], [38], [46]

$$C_2^{\text{upper}} = \underbrace{\sum_{i=1}^{\alpha} p_i \log_2\left[\frac{1}{\sum_{j=1}^{\alpha} p_j e^{-B_{i,j}}}\right]}_{I^{\text{upper}}\left(a^k; Y^k\right)}, \qquad (26)$$

and

$$C_2^{\text{lower}} = \underbrace{\sum_{i=1}^{\alpha} p_i \log_2\left[\frac{1}{\sum_{j=1}^{\alpha} p_j D_{i,j}}\right]}_{I^{\text{lower}}\left(a^k; Y^k\right)}, \qquad (27)$$

respectively, where $B_{i,j}$ and $D_{i,j}$ are given by

$$B_{i,j} = \ln \frac{1 + \gamma \sum_{k=1}^{K} \|\tilde{H}_j^k\|^2}{1 + \gamma \|\tilde{H}_i\|^2} + \frac{\gamma \sum_{k=1}^{K}\left(\|\tilde{H}_i^k\|^2 - \|\tilde{H}_j^k\|^2\right)}{1 + \gamma \|\tilde{H}_j\|^2}$$

$$+ \frac{\gamma^2 \sum_{k=1}^{K}\left(\|\tilde{H}_i^k\|^2 \|\tilde{H}_j^k\|^2 - \|\left(\tilde{H}_i^k\right)^H \tilde{H}_j^k\|^2\right)}{1 + \gamma \sum_{k=1}^{K} \|\tilde{H}_j\|^2}, \qquad (28)$$

and

$$D_{i,j} = \frac{\sqrt{\left(1 + \gamma \sum_{k=1}^{K} \|\tilde{H}_i^k\|^2\right)\left(1 + \gamma \sum_{k=1}^{K} \|\tilde{H}_j^k\|^2\right)}}{\left(1 + \dfrac{\gamma \sum_{k=1}^{K}\left(\|\tilde{H}_i\|^2 + \|\tilde{H}_j\|^2\right)}{2} + \dfrac{\gamma^2 \sum_{k=1}^{K}\left(\|\tilde{H}_i^k\|^2 \|\tilde{H}_j^k\|^2 - \|\left(\tilde{H}_i^k\right)^H \tilde{H}_j^k\|^2\right)}{4}\right)}, \qquad (29)$$

respectively.

Observe in (26) and (28) that $B_{i,i} = 0$ and that $0 \leq B_{i,j} \leq 1 \ (i \neq j)$. Thus, we have $0 \leq I^{\text{upper}}\left(a^k; Y^k\right) \ \forall k \leq \sum_{i=1}^{\alpha} p_i \log_2\left[\frac{1}{p_i}\right]$, where $\sum_{i=1}^{\alpha} p_i \log_2\left[\frac{1}{p_i}\right]$ is exactly the information conveyed via the subcarrier activation pattern. Similarly, we obtain $0 \leq I^{\text{lower}}\left(a^k; Y^k\right) \leq \sum_{i=1}^{\alpha} p_i \log_2\left[\frac{1}{p_i}\right] \ \forall k$ from (27) and (29).

Fig. 5 and Fig. 6 portray the capacity bounds of $C^{\text{upper}} = \left(C_1 + C_2^{\text{upper}}\right)$ and $C^{\text{lower}} = \left(C_1 + C_2^{\text{lower}}\right)$ as given by (24), (26) and (27) using $N_b = 4$, $N_a = 2$ and the set of probabilities $\mathfrak{p} = \left\{\frac{1}{6}, \frac{1}{6}, \frac{1}{6}, \frac{1}{6}, \frac{1}{6}, \frac{1}{6}\right\}$ and $\mathfrak{p} = \left\{\frac{1}{4}, \frac{1}{4}, \frac{1}{8}, \frac{1}{8}, \frac{1}{8}, \frac{1}{8}\right\}$. As seen in Fig. 5 and Fig. 6, the upper and the lower bounds C^{upper} and C^{lower} on the capacity are tight for both the two sets of probabilities. Thus either C^{upper} or C^{lower} may be taken as a measure of $C(\mathfrak{p})$ for the optimization of the probabilities given by $\mathfrak{p}$.

B. SYMBOL ERROR RATE (SER-) OPTIMAL DESIGN

In this approach, the adaptive SIM-OFDM finds the specific set of probabilities $\mathfrak{p}$, which minimizes the SER.

Considering the system model of ((9)), the conditional pairwise symbol error probability (PSEP) of misinterpreting the transmit vector X^k corresponding to a specific subcarrier activation pattern a^k for $\tilde{X}^k$, which corresponds to another
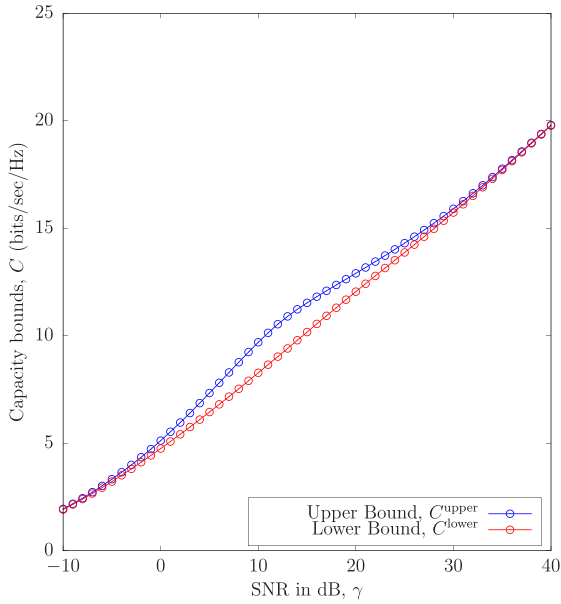
FIGURE 5. The upper as well as the lower bound on the capacity of the proposed adaptive SIM-OFDM system using $\mathfrak{p} = \left\{ \frac{1}{6}, \frac{1}{6}, \frac{1}{6}, \frac{1}{6}, \frac{1}{6}, \frac{1}{6} \right\}$. These bounds are computed for the system with $N_c = 64$, $N_b = 4$ and $N_a = 2$.
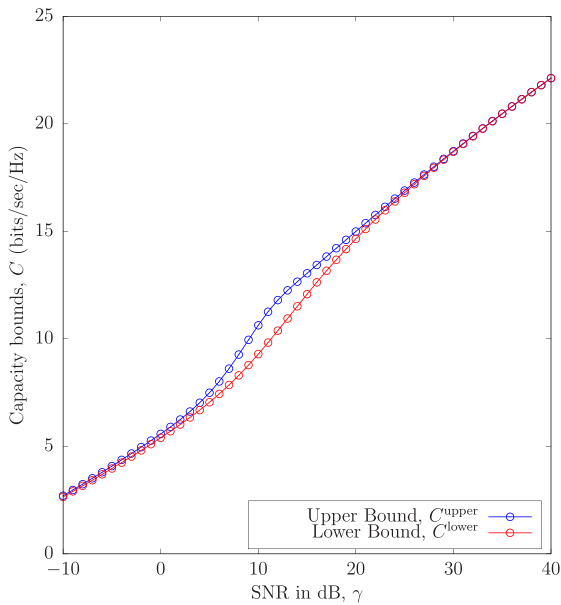

FIGURE 6. The capacity upper and lower bounds employing $\mathfrak{p} = \left\{ \frac{1}{4}, \frac{1}{4}, \frac{1}{8}, \frac{1}{8}, \frac{1}{8}, \frac{1}{8} \right\}$. Equation (24), (26) and (27) are used for calculating the bounds for the system with $N_c = 64$, $N_b = 4$ and $N_a = 2$.

subcarrier pattern $\tilde{a}^k$, may be expressed by [7]

$$\Pr\left(X^k \to \tilde{X}^k \mid \tilde{H}^k \right) = Q\left(\sqrt{\frac{d^2}{2\sigma_V^2}} \right), \quad (30)$$

where

$$d^2 = \left\| \tilde{H}^k \left(X^k - \tilde{X}^k \right) \right\|^2 = \left(\tilde{H}^k \right)^H \Lambda \tilde{H}^k \quad (31)$$

and

$$\Lambda = \left(X^k - \tilde{X}^k \right)^H \left(X^k - \tilde{X}^k \right). \quad (32)$$

Furthermore, the unconditional PSEP of misinterpreting X^k for $\tilde{X}^k$ depending on the set of probabilities $\mathfrak{p}$ may be expressed as [7]

$$
\begin{aligned}
\text{SER}(\mathfrak{p}) &= \Pr\left(X^k \to \tilde{X}^k \right) \\
&= \frac{\frac{1}{12}}{|I_{N_b} + q_1 K_{N_b} \Lambda|} + \frac{\frac{1}{4}}{|I_{N_b} + q_2 K_{N_b} \Lambda|}, \quad (33)
\end{aligned}
$$

where $q_1 = \frac{1}{(4N_0)}$, $q_2 = \frac{1}{(3N_0)}$ and K_{N_b} is defined by

$$K_{N_b} \triangleq \mathcal{E}\left\{ \left(\tilde{H}^k \right)^H \tilde{H}^k \right\}. \quad (34)$$

The optimization problem for the SER-optimal design of our adaptive SIM-OFDM may thus be formulated as

$$
\begin{aligned}
\min_{\mathfrak{p}} \ &\text{SER}(\mathfrak{p}) \\
\text{s.t.} \ &\mathfrak{p} \in \mathbb{P}. \quad (35)
\end{aligned}
$$

Specifically, we consider only the legitimate values of $\mathfrak{p}$ based on the discrete domain of (17). The sets of probabilities $\mathfrak{p} \in \mathbb{P}$ are then used for mapping the incoming index bits to the *candidate* transmit vector $\check{X}^k$. The unconditional PSEP for all these candidate $\check{X}^k$ are calculated using ((33)) and the value of $\mathfrak{p}$, which provides the minimum unconditional PSEP based on the optimization of ((35)), which is then used by the Huffman mapper to map the index bits to the subcarrier activation pattern.

C. EE-OPTIMAL DESIGN

In this section, we design Huffman mapping aided adaptive SIM-OFDM scheme by employing the probabilities $\mathfrak{p}$ gleaned from the EE optimization of the system. We adopt the 'bit-per-Joule' definition [47] of EE here, in the context of frequency-selective channels, as detailed in [48] and [49]. To be specific, the EE of our scheme is defined by the transmission data rate R per unit energy usage. The total power consumed by the transmission of a single subblock of our SIM-OFDM system may be expressed as $P_T = P_c + \frac{1}{\zeta} \sum_{n_a=1}^{N_a} P_{n_a}$, where P_c denotes the circuit power representing the average energy consumption of device electronics such as filters, digital-to-analog converters etc. excluding that of the power amplifiers involved in the transmission. Furthermore, $\zeta \in [0, 1]$ indicates the power amplifier efficiency and P_{n_a} refers to the per subcarrier signal power of $P_{n_a} = \sigma_X^2 \ \forall n_a$, which may be expressed in terms of the SNR as $P_{n_a} = \gamma N_0$. The EE of the system may thus be expressed as [21]

$$\eta_{\text{EE}} = \frac{R}{P_c + \frac{1}{\zeta} \sum_{n_a=1}^{N_a} P_{n_a}}. \quad (36)$$

Since the achievable rate of the system may be expressed in terms of the mutual information given by (23) and as the upper and the lower bounds on the capacity given by $\left(C_1 + C_2^{\text{upper}}\right)$ and $\left(C_1 + C_2^{\text{lower}}\right)$ are tight, we may consider the transmission rate to be equal to $W\left(C_1 + C_2^{\text{lower}}\right)$. Thus, considering equal EE performance for each of the K parallel blocks, we have

$$\eta_{\text{EE}} = \frac{W \sum_{i=1}^{\alpha} p_i \log_2\left(1 + \gamma \|\tilde{\boldsymbol{H}}_i^k\|^2\right) + W \sum_{i=1}^{\alpha} p_i \log_2\left(\frac{1}{\sum_{j=1}^{\alpha} p_j D_{i,j}}\right)}{P_c + \frac{N_a \gamma N_0}{\zeta}}. \quad (37)$$

Alternatively, considering the upper bound of the capacity as a measure of the data rate, the EE of the system may be defined as:

$$\eta_{\text{EE}} = \frac{W \sum_{i=1}^{\alpha} p_i \log_2\left(1 + \gamma \|\tilde{\boldsymbol{H}}_i^k\|^2\right) + W \sum_{i=1}^{\alpha} p_i \log_2\left(\frac{1}{\sum_{j=1}^{\alpha} p_j e^{-B_{i,j}}}\right)}{P_c + \frac{N_a \gamma N_0}{\zeta}}. \quad (38)$$

Having defined the EE in terms of the probabilities p_i either in (37) or in (38), the optimum set $\mathfrak{p}$ of probabilities may be obtained by solving

$$\min_{\mathfrak{p}} \eta_{\text{EE}}(\mathfrak{p})$$
$$\text{s.t. } \mathfrak{p} \in \mathbb{P}. \quad (39)$$

The optimized set $\mathfrak{p}$ of probabilities may now be used for mapping the index bits to the subcarrier activation patterns of (6) by the Huffman coding aided principle.

V. NUMERICAL RESULTS

In this section, we numerically characterize our entropy-coding assisted adaptive SIM-OFDM system in terms of its capacity, BER and EE.

A. CAPACITY

We investigate the information theoretic capacity of the proposed adaptive SIM-OFDM system in Fig. 7 employing a set of equal probabilities of $\mathfrak{p} = \left\{\frac{1}{6}, \frac{1}{6}, \frac{1}{6}, \frac{1}{6}, \frac{1}{6}, \frac{1}{6}\right\}$ as well as a second set of $\mathfrak{p} = \left\{\frac{1}{4}, \frac{1}{4}, \frac{1}{8}, \frac{1}{8}, \frac{1}{8}, \frac{1}{8}\right\}$ and using the optimization of (18). The capacity C as given by (23) is shown for the above-mentioned probabilities and the capacity C_1 as given by (24) is also shown. This gives us an idea of how the total capacity C is divided between the capacity
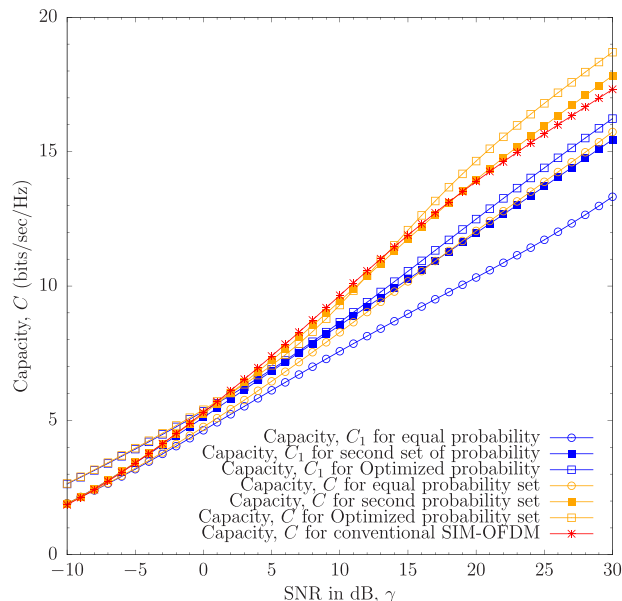

FIGURE 7. Capacity of the proposed SIM-OFDM system in dispersive COST207-RA channels having a normalized Doppler frequency of $f_d = 0.01$. The capacity of the proposed scheme is computed under different scenario as listed in Table 3 and employing a set of equal probabilities of $\mathfrak{p} = \left\{\frac{1}{6}, \frac{1}{6}, \frac{1}{6}, \frac{1}{6}, \frac{1}{6}, \frac{1}{6}\right\}$ as well as a second set of $\mathfrak{p} = \left\{\frac{1}{4}, \frac{1}{4}, \frac{1}{8}, \frac{1}{8}, \frac{1}{8}, \frac{1}{8}\right\}$ and is compared with that of the classic SIM-OFDM benchmarker.

of the constellation symbols C_1 and the capacity C_2 of the subcarrier indices. The capacity of the classic SIM-OFDM system of [7], [9], and [13] is also shown as a benchmarker. We observe that our adaptive SIM-OFDM scheme outperforms the classic SIM-OFDM scheme. This is because we are capable of adaptively selecting the best set of probabilities with the aid of the Huffman variable-length mapping, whereas the conventional SIM-OFDM scheme only employs the equal-probability scenario. In addition, the variable-length codebook facilitates the employment of all the legitimate $\binom{N_b}{N_a}$ subcarrier activation patterns, while the classic SIM-OFDM system can only cater for $2^{\left\lfloor \log_2 \binom{N_b}{N_a} \right\rfloor}$ number of patterns to be activated.

B. BIT ERROR PERFORMANCE

Fig. 8 portrays the BER of the proposed adaptive SIM-OFDM system employing both the ML detector of Section II-C.1 and the soft-decision LLR detector of Section II-C.2. We have considered the dispersive COST207-RA channel model of [49] having a normalized Doppler frequency of $f_d = 0.01$. The main simulation parameters of this invesigation are listed in Table 3. We have considered both BPSK and QPSK modulation with the aid of $N_c = 64$ OFDM subcarriers and CPs of appropriate length were appended to each OFDM symbol in order to eliminate the intersysmbol interference (ISI). Observe that the LLR detector provides a performance similar to that attained by the ML detector. This is because the LLRs defined by (13) for the soft-decision detector are expressed in terms of the ML metric of

TABLE 3. Main simulation parameters.

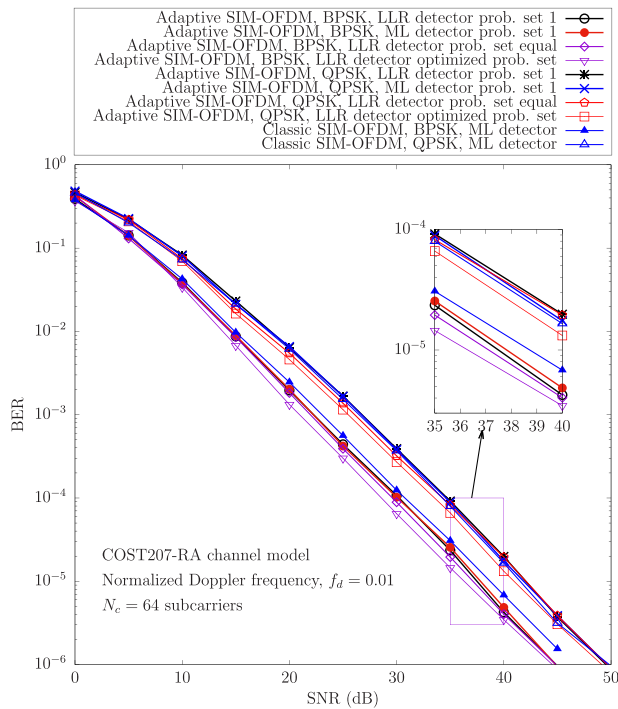|	
Channel model	COST207-RA
Fast fading envelope	Rayleigh
Normalized Doppler frequency	0.01
No. of subcarriers, N_c	64
Carrier center frequency	2.5 GHz
Subcarrier bandwidth	64 KHz
Noise spectral density N_0	-130 dBm/Hz
CP length	32
Modulation order, $\mathcal{L}$	2/ 4
Number of parallel subblocks, K	16
Circuit Power P_c	100 mW=0.1 J/sec
Power amplifier efficiency ζ	0.8

FIGURE 8. Bit-error-performance of the proposed adaptive SIM-OFDM system in conjunction with the $\mathcal{L}$−ary modulation in dispersive COST207-RA channels having a normalized Doppler frequency of $f_d = 0.01$ employing both the ML detector and the reduced-complexity soft-decision detector of Section II-C.1 and Section II-C.2 respectively. The performance with different probability set as well as an optimized set of probabilities are shown and are compared with those of the corresponding classic SIM-OFDM benchmarkers.
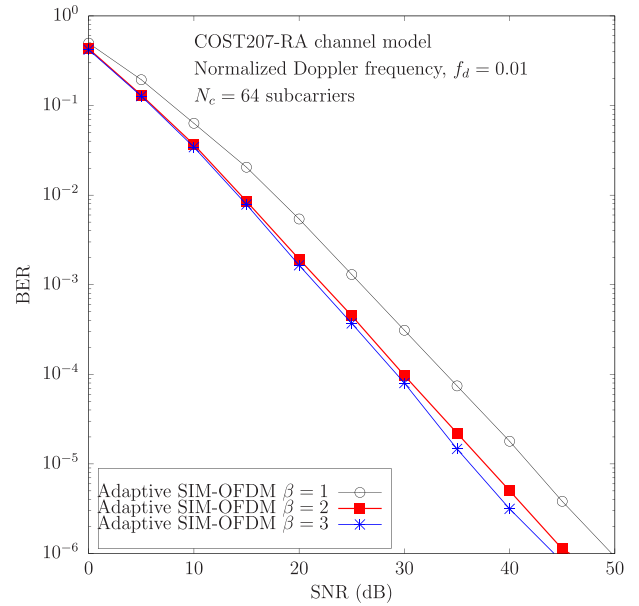

FIGURE 9. The bit-error-ratio performance of the proposed adaptive SIM-OFDM system is investigated for different probability search depths as given by β of (17).
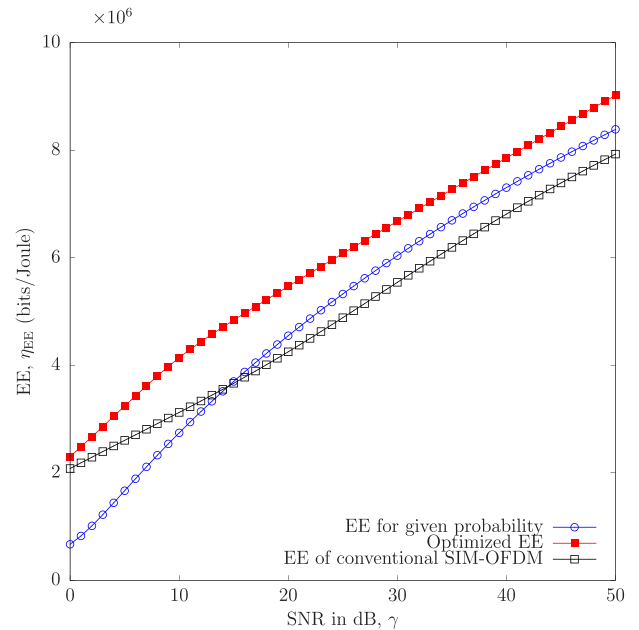

FIGURE 10. The EE of the adaptive SIM-OFDM scheme employing the probability set of $\mathbf{p} = \left\{ \frac{1}{4}, \frac{1}{4}, \frac{1}{8}, \frac{1}{8}, \frac{1}{8}, \frac{1}{8} \right\}$ as well as with the optimized set of probabilities are shown against that of the conventional SIM-OFDM scheme. Our optimized adaptive SIM-OFDM scheme outperforms the classic SIM-OFDM scheme of [7] and [9].

minimizing the error probability, which depends on the Euclidean distance between any two symbols. We observe that our scheme provides a better BER performance than its classic SIM-OFDM counterpart, especially when appropriately optimized.

To compare the performance for different probability search depths as given by β of (17), we have investigated the BER performance of the proposed adaptive SIM-OFDM system in Fig. 9. To be specific, since we have considered

$N_b = 4$, $N_a = 2$, we have $\alpha = \binom{4}{2} = 6$ and hence we can consider $p_i = 0, 1, 1/2, 1/4, 1/8, 1/6, 1/3$ from (17). Using these values, the legitimate set of probabilities can be considered, while ensuring that $\sum_{i=1}^{6} p_i = 1$. Using a lower β value will give us a lower number of probability set. However, reducing β and the associated number of probability

sets may degrade the performance. Fig. 9 illustrates the BER performance of our proposed adaptive SIM-OFDM system for $\beta = 1, 2, 3$. We observe that reducing β from 3 to 2 does not significantly degrade the performance under this specific scenario, but an excessive reduction of β leading to having only a few sets pf probabilities is expected to degrade the performance.

C. ENERGY-EFFICIENCY

In Fig. 10, we have investigated the EE of our proposed adaptive SIM-OFDM system as given by (37). We adopted the parameters listed in Table 3 and considered the set of probabilities $\mathfrak{p} = \left\{ \frac{1}{4}, \frac{1}{4}, \frac{1}{8}, \frac{1}{8}, \frac{1}{8}, \frac{1}{8} \right\}$ in Fig. 10. We also show the EE of the optimized adaptive SIM-OFDM against that of the classic SIM-OFDM system. We observe that the adaptive SIM-OFDM scheme is capable of outperforming both the classic SIM-OFDM of [7], [9], and [13] as well as the fixed-probability scheme in terms of its EE.

VI. CONCLUSIONS

In this paper, we proposed a novel adaptive subcarrier index modulated OFDM system with the aid of the Huffman entropy coding principle. The source information is mapped to the subcarriers of an OFDM system as well as to the indices of the subcarriers activated like in the SIM-OFDM system. However, rather than mapping the index bits equiprobably to the subcarrier activation patterns, we map them using specific probabilities gleaned from an optimization procedure. These probabilties are then employed by Huffman coding for generating a codebook in order to map the index information bits to the subcarriers activated. The employment of the variable-length codebook has the advantage that we are capable of employing all the legitimate patterns of subcarriers to be activated, while the conventional SIM-OFDM schemes can only use a subset of these patterns. Additionally, the probability used in Huffman coding can be adaptively chosen in order to optimize either the channel capacity, or the error performance, or alternatively the EE of the system. A pareto-optimal design of the adaptive SIM-OFDM system constitutes a promising open problem for future study.

REFERENCES

[1] R. W. Chang, "Synthesis of band-limited orthogonal signals for multichannel data transmission," *Bell Syst. Tech. J., The*, vol. 45, no. 10, pp. 1775–1796, Dec. 1966.

[2] S. Weinstein and P. Ebert, "Data transmission by frequency-division multiplexing using the discrete Fourier transform," *IEEE Trans. Commun. Technol.*, vol. 19, no. 5, pp. 628–634, Oct. 1971.

[3] *Radio Broadcasting Systems: Digital Audio Broadcasting (DAB) to Mobile, Portable and Fixed Receivers*, document ETSI EN 300 401, ETSI, May 1997.

[4] *Digital Video Broadcasting: Framing Structure, Channel Coding, and Modulation for Digital Terrestrial Television*, document ETSI EN 300 744, ETSI, Aug. 1997.

[5] *IEEE Standard for Wireless LAN Medium Access Control (MAC) and Physical (PHY) Layer Specifications*, IEEE Standard 802.11, IEEE LAN/MAN Standards Committee, Nov. 1997.

[6] P. K. Frenger and N. A. B. Svensson, "Parallel combinatory OFDM signaling," *IEEE Trans. Commun.*, vol. 47, no. 4, pp. 558–567, Apr. 1999.

[7] E. Başar, U. Aygölü, E. Panayırcı, and H. V. Poor, "Orthogonal frequency division multiplexing with index modulation," *IEEE Trans. Signal Process.*, vol. 61, no. 22, pp. 5536–5549, Nov. 2013.

[8] E. Basar, "On multiple-input multiple-output OFDM with index modulation for next generation wireless networks," *IEEE Trans. Signal Process.*, vol. 64, no. 15, pp. 3868–3878, Aug. 2016.

[9] N. Ishikawa, S. Sugiura, and L. Hanzo, "Subcarrier-index modulation aided OFDM—Will it work?" *IEEE Access*, vol. 4, pp. 2580–2593, 2016.

[10] N. Kitamoto and T. Ohtsuki, "Parallel combinatory multiple-subcarrier optical wireless communication systems," *Int. J. Commun. Syst.*, vol. 18, no. 3, pp. 195–203, 2005.

[11] Y. Hou and M. Hamamura, "A novel modulation with parallel combinatory and high compaction multi-carrier modulation," *IEICE Trans. Fundam. Electron. Commun. Comput. Sci.*, vol. E90-A, no. 11, pp. 2556–2567, Nov. 2007.

[12] Y. Hou and T. Hase, "New OFDM structure with parallel combinatory code," *IEEE Trans. Consum. Electron.*, vol. 55, no. 4, pp. 1854–1859, Nov. 2009.

[13] R. Abu-Alhiga and H. Haas, "Subcarrier-index modulation OFDM," in *Proc. IEEE Int. Symp. Pers., Indoor, Mobile Radio Commun.*, Tokyo, Japan, Sep. 2009, pp. 177–181.

[14] M. Wen, X. Cheng, M. Ma, B. Jiao, and H. V. Poor, "On the achievable rate of OFDM with index modulation," *IEEE Trans. Signal Process.*, vol. 64, no. 8, pp. 1919–1932, Apr. 2016.

[15] E. Başar, "Multiple-input multiple-output OFDM with index modulation," *IEEE Signal Process. Lett.*, vol. 22, no. 12, pp. 2259–2263, Dec. 2015.

[16] R. Y. Mesleh, H. Haas, S. Sinanovic, C. W. Ahn, and S. Yun, "Spatial modulation," *IEEE Trans. Veh. Technol.*, vol. 57, no. 4, pp. 2228–2241, Jul. 2008.

[17] M. Di Renzo, H. Haas, A. Ghrayeb, S. Sugiura, and L. Hanzo, "Spatial modulation for generalized MIMO: Challenges, opportunities and implementation," *Proc. IEEE*, vol. 102, no. 1, pp. 56–103, Jan. 2014.

[18] Y. Yang and B. Jiao, "Information-guided channel-hopping for high data rate wireless communication," *IEEE Commun. Lett.*, vol. 12, no. 4, pp. 225–227, Apr. 2008.

[19] H. Zhang, L.-L. Yang, and L. Hanzo, "Compressed sensing improves the performance of subcarrier index-modulation-assisted OFDM," *IEEE Access*, vol. 4, pp. 7859–7873, Oct. 2016.

[20] C.-B. Chae, A. Forenza, R. W. Heath, Jr., M. R. McKay, and I. B. Collings, "Adaptive MIMO transmission techniques for broadband wireless communication systems [topics in wireless communications]," *IEEE Commun. Mag.*, vol. 48, no. 5, pp. 112–118, May 2010.

[21] G. Miao, N. Himayat, and G. Y. Li, "Energy-efficient link adaptation in frequency-selective channels," *IEEE Trans. Commun.*, vol. 58, no. 2, pp. 545–554, Feb. 2010.

[22] S. Sanayei and A. Nosratinia, "Antenna selection in MIMO systems," *IEEE Commun. Mag.*, vol. 42, no. 10, pp. 68–73, Oct. 2004.

[23] A. F. Molisch, M. Z. Win, Y.-S. Choi, and J. H. Winters, "Capacity of MIMO systems with antenna selection," *IEEE Trans. Wireless Commun.*, vol. 4, no. 4, pp. 1759–1772, Jul. 2005.

[24] M. Di Renzo and H. Haas, "Improving the performance of space shift keying (SSK) modulation via opportunistic power allocation," *IEEE Commun. Lett.*, vol. 14, no. 6, pp. 500–502, Jun. 2010.

[25] R. Y. Chang, S.-J. Lin, and W.-H. Chung, "Energy efficient transmission over space shift keying modulated MIMO channels," *IEEE Trans. Commun.*, vol. 60, no. 10, pp. 2950–2959, Oct. 2012.

[26] X. Wu, M. D. Renzo, and H. Haas, "Adaptive selection of antennas for optimum transmission in spatial modulation," *IEEE Trans. Wireless Commun.*, vol. 14, no. 7, pp. 3630–3641, Jul. 2015.

[27] P. Yang, Y. Xiao, Y. Yu, and S. Li, "Adaptive spatial modulation for wireless MIMO transmission systems," *IEEE Commun. Lett.*, vol. 15, no. 6, pp. 602–604, Jun. 2011.

[28] R. Rajashekar, K. V. S. Hari, and L. Hanzo, "Antenna selection in spatial modulation systems," *IEEE Commun. Lett.*, vol. 17, no. 3, pp. 521–524, Mar. 2013.

[29] A. Czylwik, "Adaptive OFDM for wideband radio channels," in *Proc. IEEE GLOBECOM*, vol. 1. Nov. 1996, pp. 713–718.

[30] L. Hanzo, M. Munster, B. J. Choi, and T. Keller, *OFDM and MC-CDMA for Broadband Multi-User Communications, WLANs and Broadcasting*. New York, NY, USA: Wiley, 2003.

[31] T. Keller and L. Hanzo, "Adaptive multicarrier modulation: A convenient framework for time-frequency processing in wireless communications," *Proc. IEEE*, vol. 88, no. 5, pp. 611–640, May 2000.

[32] Y.-S. Shin, C. Mun, J. G. Yook, Y.-J. Yoon, and H.-K. Park, "Capacity maximising efficient adaptive subcarrier selection in OFDM with limited feedback," *Electron. Lett.*, vol. 42, no. 7, pp. 430–431, Mar. 2006.

[33] G. Song and Y. Li, "Cross-layer optimization for OFDM wireless networks—Part I: Theoretical framework," *IEEE Trans. Wireless Commun.*, vol. 4, no. 2, pp. 614–624, Mar. 2005.

[34] C. Y. Wong, R. S. Cheng, K. B. Lataief, and R. D. Murch, "Multiuser OFDM with adaptive subcarrier, bit, and power allocation," *IEEE J. Sel. Areas Commun.*, vol. 17, no. 10, pp. 1747–1758, Oct. 1999.

[35] W.-C. Pao, Y.-F. Chen, and M.-G. Tsai, "An adaptive allocation scheme in multiuser OFDM systems with time-varying channels," *IEEE Trans. Wireless Commun.*, vol. 13, no. 2, pp. 669–679, Feb. 2014.

[36] Q. Ma, Y. Xiao, L. Dan, P. Yang, L. Peng, and S. Li, "Subcarrier allocation for OFDM with index modulation," *IEEE Commun. Lett.*, vol. 20, no. 7, pp. 1469–1472, Jul. 2016.

[37] D. A. Huffman, "A method for the construction of minimum-redundancy codes," *Proc. Inst. Radio Eng.*, vol. 40, no. 9, pp. 1098–1101, Sep. 1952.

[38] W. Wang and W. Zhang, "Huffman coding based adaptive spatial modulation," *IEEE Trans. Wireless Commun.*, vol. 16, no. 8, pp. 5090–5101, Aug. 2017.

[39] A. Younis, N. Serafimovski, R. Mesleh, and H. Haas, "Generalised spatial modulation," in *Proc. Asilomar Conf. Signals, Syst., Comput.*, Nov. 2010, pp. 1498–1502.

[40] S. Sugiura, S. Chen, and L. Hanzo, "Generalized space-time shift keying designed for flexible diversity-, multiplexing- and complexity-tradeoffs," *IEEE Trans. Wireless Commun.*, vol. 10, no. 4, pp. 1144–1153, Apr. 2011.

[41] L. Cimini, Jr., "Analysis and simulation of a digital mobile channel using orthogonal frequency division multiplexing," *IEEE Trans. Commun.*, vol. 33, no. 7, pp. 665–675, Jul. 1985.

[42] G. L. Stüber, J. R. Barry, S. W. McLaughlin, Y. Li, M. A. Ingram, and T. G. Pratt, "Broadband MIMO-OFDM wireless communications," *Proc. IEEE*, vol. 92, no. 2, pp. 271–294, Feb. 2004.

[43] J. P. Woodard and L. Hanzo, "Comparative study of turbo decoding techniques: An overview," *IEEE Trans. Veh. Technol.*, vol. 49, no. 6, pp. 2208–2233, Nov. 2000.

[44] S. ten Brink, J. Speidel, and R.-H. Yan, "Iterative demapping and decoding for multilevel modulation," in *Proc. IEEE Global Telecommun. Conf. (GLOBECOM)*, vol. 1. Nov. 1998, pp. 579–584.

[45] P. Robertson, E. Villebrun, and P. Hoeher, "A comparison of optimal and sub-optimal MAP decoding algorithms operating in the log domain," in *Proc. IEEE Int. Conf. Commun. (ICC)*, vol. 2. Jun. 1995, pp. 1009–1013.

[46] Z. An, J. Wang, J. Wang, S. Huang, and J. Song, "Mutual information analysis on spatial modulation multiple antenna system," *IEEE Trans. Commun.*, vol. 63, no. 3, pp. 826–843, Mar. 2015.

[47] Y. Chen *et al.*, "Fundamental trade-offs on green wireless networks," *IEEE Commun. Mag.*, vol. 49, no. 6, pp. 30–37, Jun. 2011.

[48] S. Verdú, "Spectral efficiency in the wideband regime," *IEEE Trans. Inf. Theory*, vol. 48, no. 6, pp. 1319–1343, Jun. 2002.

[49] "Digital land mobile radio communications, final report," European Communities, Luxembourg, Tech. Rep. COST 207, 1989.

HONGMING ZHANG (S'15) received the B.Eng. degrees (Hons.) in telecommunications from the Nanjing University of Aeronautics and Astronautics and the City University of London, both in 2011, the M.Sc degree in wireless communications from the University of Southampton in 2012, and the Ph.D. degree from the University of Southampton. He joined Columbia University. His research interests include power line communications, compressed sensing, and the design of communications systems.
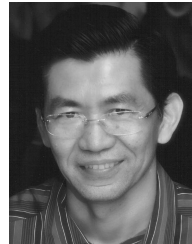
SHENG CHEN (M'90–SM'97–F'08) received the B.Eng. degree in control engineering from the East China Petroleum Institute, Dongying, China, in 1982, and the Ph.D. degree in control engineering from the City, University of London in 1986. and the D.Sc. degree, higher doctoral degree, from the University of Southampton, Southampton, U.K.

From 1986 to 1999, He held research and academic appointments with The Universities of Sheffield, The Universities of Edinburgh, and the Universities of Portsmouth, all in U.K. Since 1999, he has been with the School of Electronics and Computer Science, University of Southampton, U.K., where he currently a Professor in intelligent systems and signal processing. He has published over 500 research papers. His research interests include adaptive signal processing, wireless communications, modelling and identification of nonlinear systems, neural network and machine learning, intelligent control system design, evolutionary computation methods, and optimization.

Dr. Chen is a Fellow of IET, a Distinguished Adjunct Professor with King Abdulaziz University, Jeddah, Saudi Arabia, and an ISI Highly Cited Researcher in engineering (2004). In 2014, he was elected as a Fellow of the United Kingdom Royal Academy of Engineering.

LAJOS HANZO (M'91–SM'92–F'04) received the D.Sc. degree in electronics in 1976 and the Ph.D. degree in 1983. During his 40-year career in telecommunications, he has held various research and academic posts in Hungary, Germany, and U.K. Since 1986, he has been with the School of Electronics and Computer Science, University of Southampton, U.K. He is currently directing a 60-strong academic research team, working on a range of research projects in the field of wireless multimedia communications sponsored by industry, the Engineering and Physical Sciences Research Council, U.K., the European Research Council's Advanced Fellow Grant, and the Royal Society's Wolfson Research Merit Award. He is an enthusiastic supporter of industrial and academic liaison and he offers a range of industrial courses. He has successfully supervised 111 Ph.D. students, co-authored 18 John Wiley/IEEE Press books on mobile radio communications totaling in excess of 10 000 pages, published 1701 research contributions at the IEEE Xplore. He has over 30 000 citations and an H-index of 72. He was a FREng, FIET, and Fellow of the EURASIP. He received an Honorary Doctorate from the Technical University of Budapest in 2009 and The University of Edinburgh in 2015. In 2016, he was admitted to the Hungarian Academy of Science. He is a Governor of the IEEE VTS. He served as the TPC Chair and the General Chair of the IEEE conferences, presented keynote lectures and has been received a number of distinctions. He is the Chair in telecommunications with the University of Southampton. From 2008 to 2012, he was an Editor-in-Chief of the IEEE Press and a Chaired Professor at Tsinghua University, Beijing.

MOHAMMAD ISMAT KADIR received the B.Sc.Eng. degree (Hons.) in electrical and electronic engineering and the M.Sc.Eng. degree in computer engineering from the Bangladesh University of Engineering and Technology, Dhaka, Bangladesh, in 1992 and 1999, respectively, and the Ph.D. degree in electronics and electrical engineering from the Communications Research Group, School of Electronics and Computer Science (ECS), University of Southampton, U.K., in 2014 He received the Commonwealth Scholarship from the Commonwealth Scholarship Commission, U.K.

Dr. Kadir is currently a Faculty Member with the Electronics and Communication Engineering Discipline, Khulna University, Bangladesh. He was a Visiting Fellow with the School of ECS, University of Southampton, from 2016 to 2017. His research interests include multi-carrier systems, space-time coding, cooperative communications, millimeter-wave communications, and heterogeneous networks.

• • •